Available online at www.sciencedirect.com
ScienceDirect
Trans. Nonferrous Met. Soc. China 29(2019) 1017−1025
Transactions of Nonferrous Metals Society of China
www.tnmsc.cn

Microstructure characteristics of Ti−43Al alloy during twin-roll strip casting and heat treatment

Mang XU, Guo-huai LIU, Tian-rui LI, Bing-xing WANG, Zhao-dong WANG

State Key Laboratory of Rolling and Automation, Northeastern University, Shenyang 110819, China

Received 7 May 2018; accepted 7 January 2019

Abstract: To shorten the fabrication process of difficult-to-form TiAl sheets, twin-roll strip casting and microstructural control were investigated in Ti−43Al alloy. A crack-free sheet with dimensions of 1000 mm × 110 mm × 2 mm was obtained. The microstructure of stip casting sheets and heat treatments was systematically studied. The macrostructure consisted of columnar crystals extending inward and centrally located equiaxed crystals with severe Al segregation were observed along the thickness direction, due to the symmetrical solidification process and decreasing cooling rates. The strip casting alloy was characterized by fine duplex microstructure with a grain spacing of 20−30 μm and a lamellar spacing of 10−20 nm. Furthermore, multiple microstructures of near gamma, nearly lamellar and fully lamellar were obtained through heat treatment process with significantly improved homogeneity of the microstructure.

Key words: strip casting; TiAl alloy; sheet fabrication; microstructure characterization; heat treatment

1 Introduction

TiAl-based alloys are viable candidates for high temperature structural applications due to their low density, good high-temperature strength and creep resistance [1−4]. TiAl sheets have been extensively used in aerospace components including hollow turbine blades, aero engine exhaust nozzles and honeycomb structures [5]. However, poor high temperature deformability combined with low ductility at room temperature makes it challenging to obtain TiAl sheets using conventional rolling technology, resulting in expensive production cost of TiAl components [6]. In the past three decades, manufacturing of γ-TiAl alloys has made remarkable progress, and intensive work has been carried out to produce crack-free γ-TiAl sheets [7−9]. Hot rolling is considered as the most efficient method to fabricate TiAl sheets with good mechanical properties. Several research efforts have been directed towards the fabrication of TiAl sheets by hot pack rolling [6,10,11]. Nevertheless, there still exist challenges in obtaining fine microstructures and good surface quality with crack-free sheets [10].

Currently, strip casting with a near-net-shape technology can be used for TiAl sheet fabrication. It involves directly casting molten metal into few millimeter-thick metal strips, thereby minimizing subsequent machining processes [12,13]. This approach has been widely used for the plate/strip production of silicon steel and aluminum alloys [14−16]. Therefore, the strip casting technique is an efficient and inexpensive method for producing large-scale TiAl sheets. Additionally, the strip casting process with the solidification and plastic deformation processes is always completed in a few seconds, which is prone to complex microstructure evolution, phase transition and solute segregation of TiAl alloys. Its near-rapid solidification characteristics (10^2−10^3 °C/s) by the copper roller may significantly change TiAl phase diagram, leading to a solidification behavior different from binary TiAl alloys under the non-equilibrium conditions. JOHNSON et al [17] showed that the competitive growth of the solidification process exists under different cooling conditions in Ti−47Al alloy. Herein, the primary α solidification process can be replaced with the primary β dendritic growth with increasing cooling rate, leading to a different phase transition and final microstructure

Foundation item: Project (51504060) supported by the National Natural Science Foundation of China; Projects (2016YFB0301201, 2016YFB0300603) supported by the National Key Research and Development Program of China; Project (N160713001) supported by the Fundamental Research Funds for the Central Universities, China

Corresponding author: Guo-huai LIU; Tel: +86-24-83686739; E-mail: liugh@ral.neu.edu.cn

DOI: 10.1016/S1003-6326(19)65010-7

morphology. KIM et al [18] indicated that the improved cooling conditions could change the TiAl phase diagram for promoting the $L\rightarrow\beta$ transition line in the low Al direction, thereby supporting the occurrence of $L+\beta\rightarrow\alpha$ transition and primary α solidification process. The near-rapid cooling process during the strip casting could suppress the occurrence of solute diffusion during the solidification and solid transition process, which would hinder the peritectic reaction of $L+\beta\rightarrow\alpha+\beta$ or $L+\alpha\rightarrow\alpha+\gamma$ and promote a fine lamellar structure during the $\alpha\rightarrow\alpha_2/\gamma$ transition. The near-rapid solidification process and microstructure evolution of the TiAl alloys are not well understood, which obscures the optimum design of strip-casting TiAl alloys for industrial applications.

Strip casting with the near-rapid solidification process easily leads to solute segregation and scattering of microstructures. It is also reported that the development of aluminum alloys (Al−Mg−Si, Al−Mn−Si and Al−Li−Cu) by the strip casting process is mainly restricted by central segregation, which leads to coarse-grains at the center and low stamping/forming properties [19,20]. While for TiAl alloys, studies [21] previously indicated that different segregation patterns such as *S*- and β-segregation exist in the direct cast microstructure, which changes greatly under near-rapid solidification and symmetric cooling conditions of the strip casting process. HANAMURA et al [22−24] investigated the microstructure evolution and grain refinement for the twin-roll cast TiAl−(B) alloy, and observed center segregation and shrinkage cavity in the central freezing-end region, which could not be easily removed by the optimization of strip casting parameters. So far, the microstructure distribution and its control for TiAl alloys have not been thoroughly investigated during strip casting and the subsequent treatment.

In this work, microstructure characteristics and their evolution were investigated for Ti−43Al alloy during strip casting and heat treatment. TiAl sheets were prepared with 1000 mm × 110 mm × 2 mm dimensions by strip casting technology, and the macro/microstructure, phase transition and microstructural parameters were investigated along the thickness direction. Additionally, the phase distribution, solute segregation and hardness were studied to measure the homogeneity of the strip casting Ti−43Al alloy. Furthermore, heat treatment was conducted for the microstructure control of the strip-casting TiAl sheets, during which the microstructure evolution and hardness were analyzed.

2 Experimental

TiAl sheets with a nominal composition of Ti−43.3Al were fabricated by twin-roll strip casting process, as shown in the schematic in Fig. 1(a). A selected proportion of Ti (99.95%) and Al (99.99%) was melted by vacuum induction. Before rolling process, the melt which was protected continuously by argon atmosphere, flowed through the chute homogeneously and was then poured into the molten pool composed of two rollers and the side dam. The sheet thickness was controlled by rolling gap, rolling speed, and loading force. A TiAl sheet with dimensions of 1000 mm × 110 mm × 2 mm (Fig. 1(b)) was finally obtained with casting speed of 0.6 m/s and average rolling force of 26 kN followed by direct air cooling (AC). An uneven oxidation surface could be observed with ~2.5 μm in thickness (Fig. 1(c)), mainly resulting from the interface reaction during forming and the subsequent cooling process. Additionally, the sheet surface was further descaled by mechanical polishing resulting in a substantial and sound surface, as shown in Fig. 1(d). Further heat treatments were conducted with temperature and holding time in range of 1250−1300 °C and 60−90 min followed by furnace cooling (FC). Anti-oxidation coatings were used to reduce surface oxidation.

The microstructure was characterized by scanning electron microscope (SEM) equipped with an energy dispersive spectrometer (EDS) in back-scattered electron (BSD) mode and transmission electron microscope (TEM). SEM samples were prepared to use standard

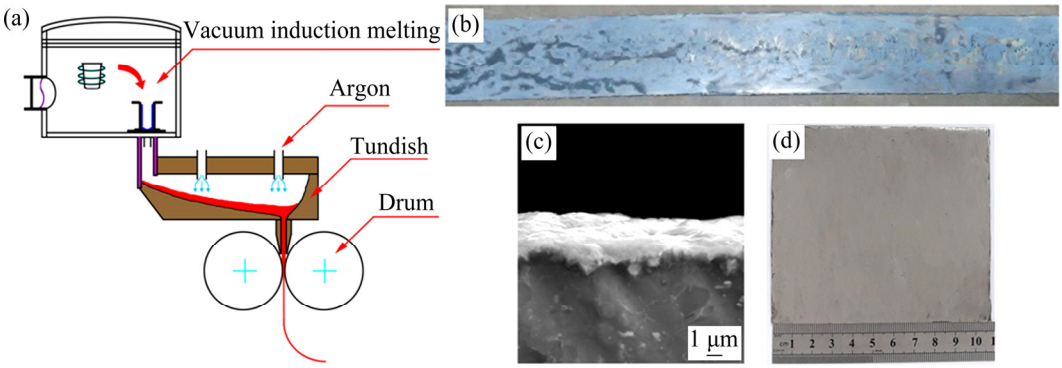

Fig. 1 Schematic diagram of twin-roll strip casting process (a), appearance of Ti−43Al sheet with dimensions of 1000 mm × 110 mm × 2 mm (b), SEM image of surface oxide layer (c) and surface quality after mechanical polishing (d)

metallographic techniques with a electrolyte formula of 100 mL $HClO_4$, 300 mL $CH_3(CH_2)_3OH$ and 500 mL CH_3OH. TEM samples were prepared by ion beam thinner. The structure and macrotexture of the as-cast sheets were determined by X-ray diffraction (XRD) on a Bruker D8 Discovery diffractometer with Co target. Samples for XRD were polished and the measuring positions along the thickness direction were the surface region and the central region. The grain size and the lamellar spacing were measured by linear intercept method using computerized image analysis. The micro-hardness along the thickness direction was measured by HV50 Vickers hardness tester.

3 Results and discussion

3.1 Macro- and microstructures of strip-casting Ti−43Al sheet

Figure 2 shows the macro- and microstructure along the thickness direction in strip-casting Ti−43Al alloy. The macrostructure contains three distinguished sections, namely, fine columnar crystal zone, coarse columnar crystal zone and central equiaxed crystal zone, as shown in Fig. 2(a). Additionally, the Al segregation in dark contrast can be observed in the center region of TiAl sheets. Due to the contact of TiAl melt with cold twin copper rollers, temperature gradient from surface to core in TiAl sheets is generated, leading to the symmetrical and centerline microstructure characteristics.

In the surface region, fine dendrites can be observed with about 2 μm spacing due to the rapid cooling, in which the second dendrites are suppressed by the compact primary dendrites, as shown in Fig. 2(b). With further solidification, the coarse dendritic growth can be observed approximately vertical to the surface in one-quarter region of TiAl sheets, and the developed primary and second dendrites are obtained mainly due to the decrease of the cooling rate, as shown in Fig. 2(c). Furthermore, the columnar to equiaxial transition (CET) blocks the dendrite growth resulting from the increased undercooling and the cracked dendritic arms in front of the solid−liquid interface. Uniform equiaxed crystals are found to be distributed in the core region of TiAl sheet, as shown in Figs. 2(d, e). These results suggest the presence of inhomogeneous microstructure distribution of TiAl sheets due to the near-rapid solidification during the strip casting process. Generally, the improved microstructure is obtained by the optimization of parameters (high rolling rate, low casting temperature and high rolling force), alloying and further mechanical treatment.

The detailed microstructure of the strip-casting Ti−43Al alloy is shown in Fig. 3. The second dendrite arms are observed to have a 60° orientation to the primary dendrites, which are suggestive of a primary α solidification process with the $L+\alpha\rightarrow\alpha$ transition according to the dendritic structure symmetry, as shown in Fig. 3(a). Vertical second dendrites accompanied with 45° or parallel α_2/γ lamellar to the growth direction are also observed, which indicates a primary β phase solidification process, as shown in Figs. 3(b, c). These results show that both of the primary α/β solidification processes exist during the strip casting process, which may be affected by the change of the cooling rate and superheating degree of TiAl melt. Additionally, according to the TiAl phase diagram, the peritectic

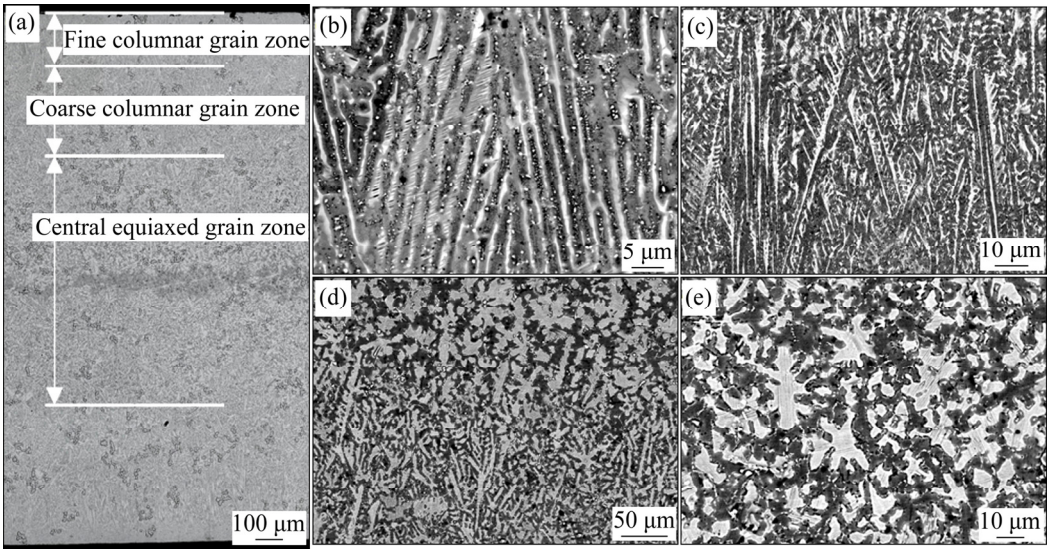

Fig. 2 Macro- and microstructure of strip-casting Ti−43Al sheet along thickness direction: (a) Macrostructure; (b) Fine columnar grain in edge region; (c) Coarse columnar grain at one-quarter region; (d) Interface of columnar to equiaxial transition; (e) Central equiaxed grain region

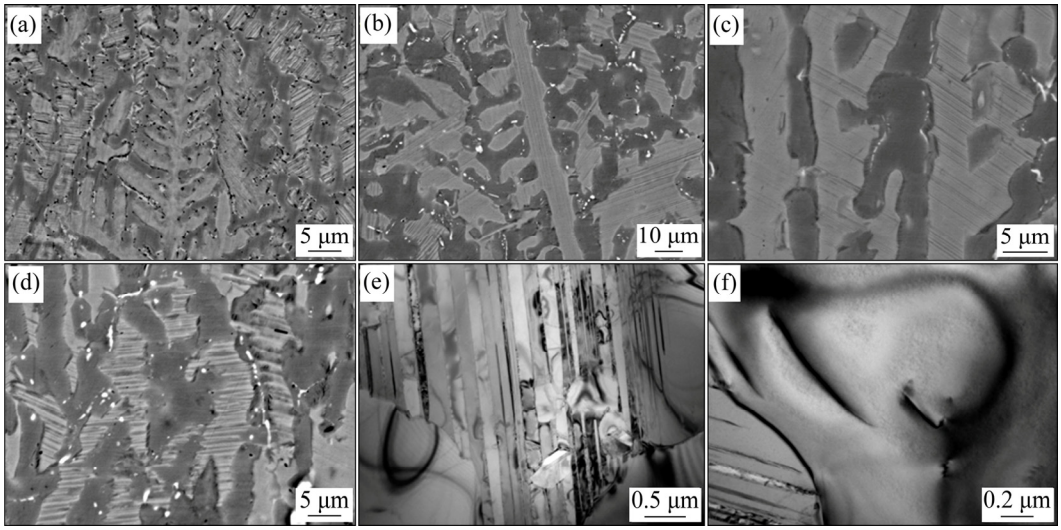

Fig. 3 Microstructures of strip-casting Ti−43Al sheets: (a) Dendritic morphology with 60° secondary arms; (b) Dendritic morphology with 90° secondary arms and parallel lamellar structure; (c) α_2/γ lamellar with 45° along growth direction; (d) Discontinuous and sliver lamellar colonies; (e) TEM micrograph for fine lamellar structure; (f) TEM micrograph of interface between (γ+α_2) lath and interdendritic γ

reaction of $L+\beta \rightarrow L+\beta+\alpha$ should occur for the selected Ti−43Al alloy. The filmy peritectic phase covering the primary β phase is also observed, and the growth of peritectic α phase is restricted by the slow solute diffusion due to the near-rapid cooling of the strip casting process, as shown in Figs. 3(b, c). Generally, the phase transition process changes significantly under the near-rapid solidification condition of the strip casting process along the thickness direction.

Discontinuous and sliver lamellar colonies are also observed in the columnar and equiaxed crystal regions, as shown in Figs. 3(b, d) and Fig. 2(e), which is suggestive of dissolution of the directional dendrites and the equiaxed α_2/γ lamellar colonies. These results are always due to the coupling effect of the near-rapid solidification and rolling process, which leads to plenty of residual stress between γ/α_2 lath and interdendritic γ phase, as shown in Figs. 3(e, f). The recrystallization and $\alpha \rightarrow \gamma$ transition can occur under the high temperature and stress conditions in strip casting TiAl alloy, during which the growth of γ lamellar may destroy the directional/ equiaxed lamellar colony during the further cooling process. These results also suggest that the increased cooling rate and rolling force may lead to the dissolution of the directional columnar crystals, which promotes the fine grains and homogeneous microstructure distribution for the strip-casting TiAl sheets.

Table 1 lists the measured lamellar spacing and grain size for the strip-casting TiAl alloys. In general, TiAl alloys prepared by conventional casting exhibit a typical full lamellar microstructure with coarse lamellar colonies, and the as-cast grain size and lamellar spacing are about 800 and 1200 nm, respectively [25,26]. However, TEM micrographs of the sheet fabricated by twin-roll strip casting show that the α_2/γ lamellar spacing is in the range of 10−20 nm, and the columnar crystal spacing is 4−15 μm while the equiaxed grain in the central region is 20−30 μm. The calculated microstructure parameters are obviously superior to those of the casting and hot deformed TiAl alloy, as listed in Table 1 [25−29], which confirms the refining effect of the strip casting. Since the discrepancy of the microstructure distribution also exists along the thickness direction, optimizing the parameters and further heat treatment are necessary to achieve homogeneous lamellar structure of the strip-casting TiAl alloys.

Table 1 Comparison of lamellar spacing and grain size of strip casting TiAl alloys with cast and hot-deformed TiAl alloys

Alloy	α_2/γ lamellar spacing/μm	Grain size/μm
Ingot	1.3	>200
As-forged	0.2−0.5	20−100
Hot-extruded	0.1	4−7.5
Strip casting	0.01−0.02	3−30

3.2 Microstructure characteristic and hardness of strip-casting Ti−43Al alloy

Figure 4 shows the XRD patterns of the columnar/equiaxed grain region and the $\{001\}_\gamma$ pole figures of the columnar region of the strip casting Ti−43Al sheet. XRD pattern indicates that the as-cast microstructure is mainly composed of γ, α_2 and TiC

phases, as shown in Fig. 4(a), in which TiC particles result from the contact reaction of the melt with the graphite crucible. It can also be observed that γ phase in the central equiaxed region is higher than that in the columnar crystal region according to its peak values. This is mainly attributed to the solute Al enrichment by the directional growth of the columnar crystals during the strip casting process. Additionally, the pole figure in Fig. 4(b) shows a weak texture of $<001>_\gamma$ axis perpendicular to panel surface in the columnar grain region. Generally, the primary phase for the strip-casting TiAl alloys includes the α_2/γ lamellar and interdendritic γ phase, in which the α_2/γ lamellar transition is in accordance with the Blackburn orientation relationships of $\{110\}_\beta//\{0001\}_\alpha//\{111\}_\gamma$ and $<111>_\beta//<1120>_\alpha//<110>_\gamma$. During the strip casting process, the primary α/β solidification may lead to different orientation characteristics of the α_2/γ lamellar, as shown in Figs. 3(a−d). The interdendritic γ phase with the preferred [001] orientation develops directly from the undercooled melt due to the coupling effect of the solidification and rolling deformation. The fractured α_2/γ lamellar colony and recrystallized γ phase may then lead to the weak texture of $<001>_\gamma$ characteristic during the strip casting process.

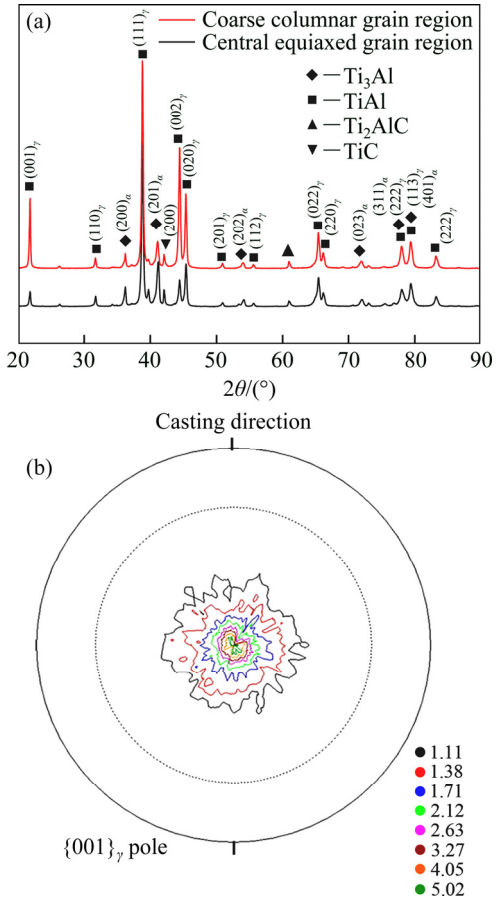

Fig. 4 XRD pattern (a) and $\{001\}_\gamma$ pole figure (b) in columnar grain region of strip-casting Ti−43Al sheet

The microstructure characteristic is further investigated by the solute distribution, grain spacing and hardness values, as shown in Fig. 5. EDS results show that the solute Al contents gradually increase from the edge to the core in Ti−43Al sheet. High Al enrichment (nearly 50 at.%) can be observed in the center region with 0.25 mm in width, while an opposite trend is observed for solute Ti distribution, as shown in Fig. 5(a). The solute distribution is closely connected with the phase transition process during the strip casting process, and the growth of both primary α and β phases promotes solute Al pushing to the front of the solid−liquid interface. As a result, the central segregation of the solute

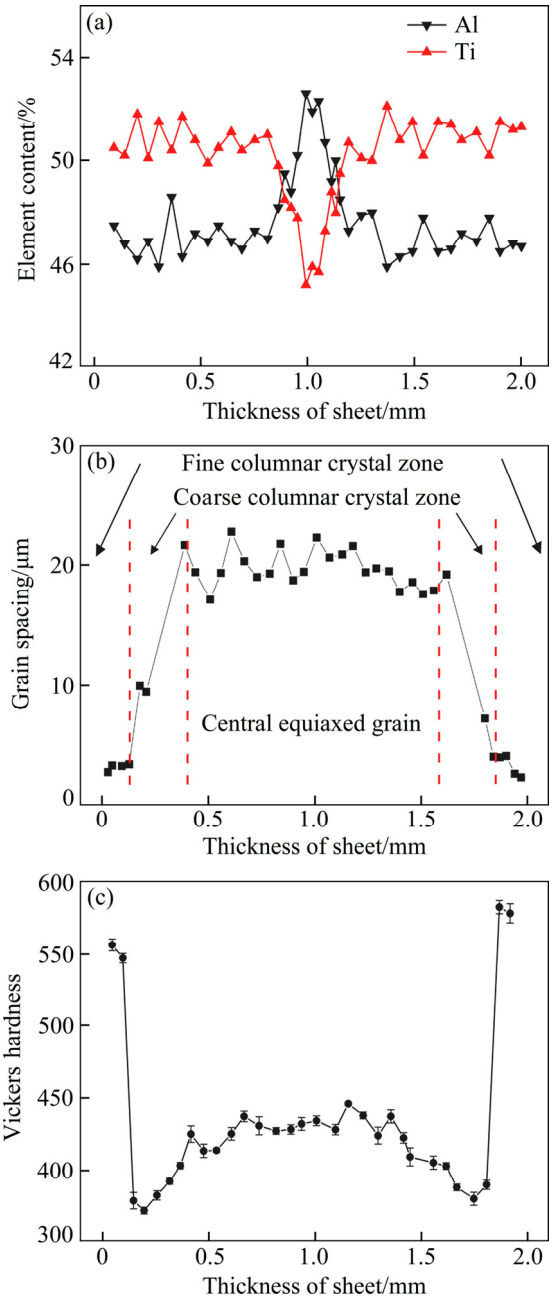

Fig. 5 Microstructure characteristic of strip-casting Ti−43Al sheets: (a) Solute distribution; (b) Grain spacing; (c) Vickers hardness

Al is obtained in the strip casting TiAl sheet, which is further increased by the symmetrical cooling conditions of the two copper rollers.

Additionally, the grain spacing and hardness values have the linear relationship with the yield stress. Figures 5(b, c) show the evolution of the grain spacing and hardness along the thickness direction. The grain spacing changes from about 10 μm in the columnar region to 20 μm in the core equiaxed region, which is mainly due to the decreasing cooling rates and microstructure discrepancy during the strip casting process. The hardness values are unusually high in the edge region and then increase gradually from the edge to the core region along the width direction. The high hardness value of HV 580 in the edge region is due to the outer chilled zone with the refined grains. While the core region has nearly HV 435, both the massive γ phase (nearly HV 200) and the coarse grain spacing characteristic may decrease the hardness values. In such cases, the high hardness can be only attributed to plenty of hard particles (TiC or oxidate) and the solution strengthening action.

According to these results, the scatter microstructure distribution and hardness can be observed along the thickness direction of the strip-casting Ti−43Al sheets. The massive γ phase, coarse grain spacing and high Al enrichment are observed in the center region due to the decreased and symmetrical cooling conditions, which seriously deteriorates the mechanical properties of the alloy. Therefore, further treatment is needed for the homogeneous microstructure in order to obtain large-scale TiAl sheets by strip casting technique. Such studies will be performed in a subsequent report.

3.3 Microstructure evolution of strip-casting Ti−43Al alloy during heat treatment process

The heat treatment process can promote solute diffusion and release the internal stress, and facilitates the control of the fine and homogeneous microstructure of the alloy. Figure 6 shows the microstructure evolution along the thickness direction with different heat treatment processes by furnace cooling (FC).

In the 1250 °C, 60 min, FC process, the central equiaxed grains gradually transform to a lump structure with the dissolution of the second arms, while the columnar grains become thin and fracture to banding structure due to the massive γ phase growth, as shown in Figs. 6(a, b). The $\alpha+\gamma$ phase region occurs within the heating temperature according to the TiAl phase diagram, and then the γ phase growth can be accelerated under the high temperature and initial stress from the strip casting process [30,31]. This promotes the dissolution of the dendrite/equiaxed α_2/γ lamellar structure**.** With the temperature increasing to 1270 °C, the near lamellar structure is first observed in the center region while the fully γ phase in the one-quarter regions is observed along the thickness direction. This mainly results from the solute distribution discrepancy, especially for the high solute Al enrichment in the center region, leading to the decrease of the $\alpha\rightarrow\alpha+\gamma$ transition process, as shown in Fig. 6(c). At 1300 °C, 60 min, FC process, an entire lamellar structure is obtained along the thickness direction, which is indicative of the occurrence of α transition temperature under the selected temperature conditions during the heat treatment process, as shown in Fig. 6(d). Simultaneously, the solute Al segregation in the center region can be eliminated due to

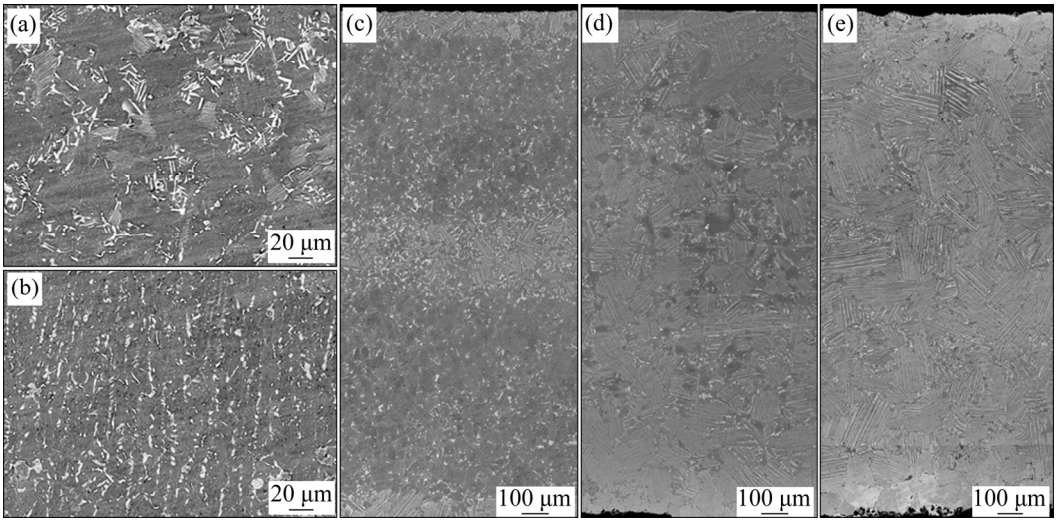

Fig. 6 Microstructure evolution of strip-casting Ti−43Al sheets treated under different conditions: Equiaxed crystals region (a) and columnar crystal region (b) after 1250 °C, 60 min, FC, showing lump and banding structures, respectively; microstructures along thickness direction at 1270 °C, 60 min, FC (c), 1300 °C, 60 min, FC (d), and 1300 °C, 90 min, FC (e)

the diffusion process. Finally, the fully α_2/γ lamellar structure is obtained along the thickness direction at 1300 °C, 90 min, FC process, which establishes that the homogeneous microstructure can be achieved by α transition treatment and the solute diffusion process, and the size of α_2/γ lamellar colony is in the range of 60−100 μm, as shown in Fig. 6(e). These results show that fully homogeneous α_2/γ lamellar structure can be obtained under the certain temperatures (near the α transition region) and holding time for the strip cast Ti−43Al alloy.

Furthermore, the hardness values measured for the strip-casting Ti−43Al alloy after the heat treatment (Fig. 7) are found to decrease as compared to the direct cast Ti−43Al sheet (Fig. 5(c)). This is indicative of decreased initial stress and the coarse microstructure. In the low heating conditions of 1250 °C, 60 min, FC and 1270 °C, 60 min, FC, wave hardness values are observed, mainly resulting from the scatter microstructure along the thickness direction. Especially in the case of 1270 °C, 60 min, FC, the high hardness is observed in the central and edge regions while the low values are observed in one-quarter region, which corresponds to the α_2/γ lamellar structure and the γ phase distribution, respectively. Additionally, homogeneous hardness distribution is obtained at the 1300 °C, FC condition, as shown in Figs. 7(c, d), which corresponds to the nearly homogeneous α_2/γ lamellar structure. These results suggest that the homogeneous microstructure and mechanical properties can be obtained after the appropriate heat treatment process.

Results indicate that the scatter microstructure and hardness can be improved during the heat treatment process, mainly through the decomposition of columnar/equiaxed crystal, $\alpha\rightarrow\gamma$ transition and solute diffusion under the high temperature and initial stress conditions. The multiple microstructure such as near α_2/γ lamellar and fully α_2/γ lamellar is obtained with the different heat treatments. Therefore, the homogeneous and required α_2/γ lamellar structure can be controlled during strip casting and the subsequent heat treatment process, thereby realizing a low-cost and high efficiency approach for large-scale sheet fabrication of TiAl alloys.

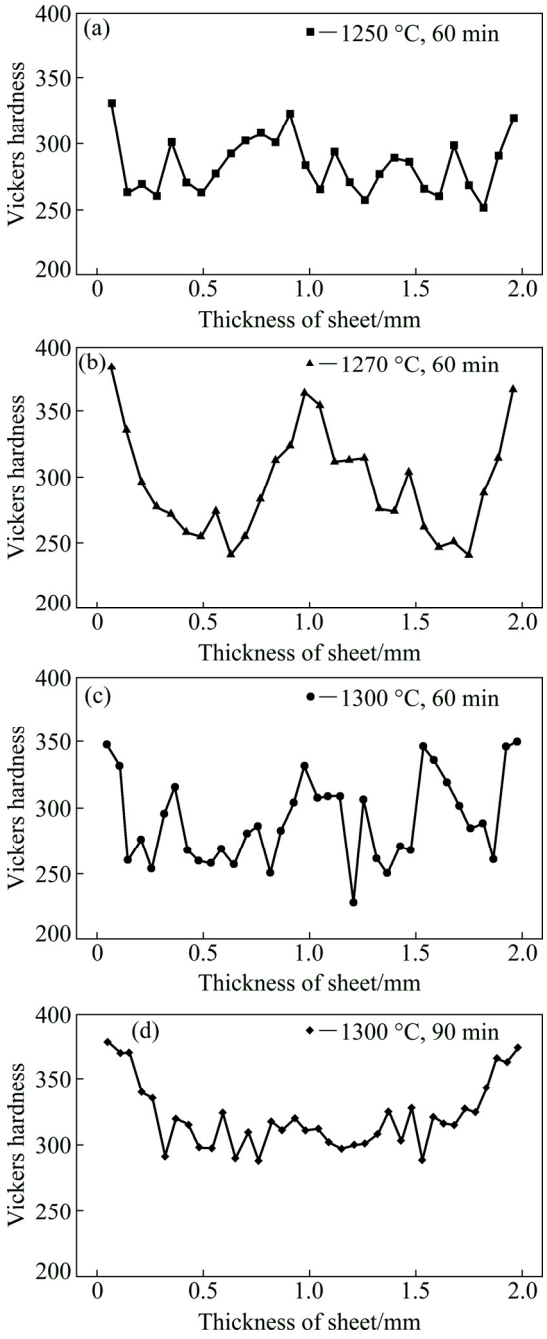

Fig. 7 Vickers hardness of strip-casting Ti−43Al sheet after different heat treatments: (a) 1250 °C, 60 min, FC; (b) 1270 °C, 60 min, FC; (c) 1300 °C, 60 min, FC; (d) 1300 °C, 90 min, FC

4 Conclusions

(1) The macrostructure with outward columnar crystals and central equiaxed crystal distribution is observed along the thickness direction along with severe Al segregation in the center region; this is mainly due to the symmetrical solidification process of primary α/β phase and the decreasing cooling rate; a fine microstructure with 10−20 nm lamellar spacing and 20−30 μm grain spacing is obtained due to the near-rapid cooling process.

(2) Scatter microstructure and hardness are observed for the strip-casting Ti−43Al sheet, and a weak preferred orientation of γ phase evolves with the $[001]_\gamma$ axis parallel to the normal direction of the sheet.

(3) Heat treatment can promote the microstructure homogeneity of the strip cast Ti−43Al alloy mainly through the decomposition of columnar and equiaxed structures; multiple microstructures of the near γ structure, nearly lamellar and fully lamellar structure can

be obtained under different temperatures and holding time; homogeneous and required α_2/γ lamellar structure can be controlled during the strip casting and subsequent heat treatment process, which enables a low-cost and high efficiency method for the large-scale sheet fabrication of TiAl alloys.

References

[1] DAS G, KESTLER H, CLEMENS H, BARTOLOTTA P A. Sheet gamma TiAl: status and opportunities [J]. Journal of Metals, 2004, 56(11): 42−45.

[2] KIM Y W. Ordered intermetallic alloys. Part Ⅲ: Gamma titanium aluminides [J]. Journal of Metals, 1994, 46(7): 30−39.

[3] LI Hui-zhong, LI Zhou, ZHANG Wei, WANG Yan, LIU Yong, WANG Hai-jun. High temperature deformability and microstructural evolution of Ti−47Al−2Cr−0.2Mo alloy [J]. Journal of Alloys and Compounds, 2010, 508(2): 359−363.

[4] LORIA E A. Gamma titanium aluminides as prospective structural materials [J]. Intermetallics, 2000, 8(9−11): 1339−1345.

[5] ZHANG Wei, LIU Yong, LIU Bin, LI Hui-zhong, TANG Bei. Deformability and microstructure transformation of PM TiAl alloy prepared by pseudo-HIP technology [J]. Transactions of Nonferrous Metals Society of China, 2010, 20(4): 547−552.

[6] LIANG Yong-feng, LIN Jun-pin. Fabrication and properties of γ-TiAl sheet materials: A review [J]. Journal of Metals, 2017, 69(12): 1−5.

[7] WEAVER M L, CALHOUN C W, GARMESTANI H. Microstructure, texture, and mechanical properties of continuously cast gamma TiAl [J]. Journal of Materials Science, 2002, 37(12): 2483−2490.

[8] WU Xin-hua. Review of alloy and process development of TiAl alloys [J]. Intermetallics, 2006, 14(10): 1114−1122.

[9] KIM Y W. Gamma titanium aluminides: Their status and future [J]. Journal of Metals, 1995, 47(7): 39−42.

[10] ZHOU Hai-tao, KONG Fan-tao, WU Kai, WANG Xiao-peng, CHEN Yu-yong. Hot pack rolling nearly lamellar Ti−44Al−8Nb−(W, B, Y) alloy with different rolling reductions: Lamellar colonies evolution and tensile properties [J]. Materials Design, 2017, 121: 202−212.

[11] LIANG Xiao-peng, LIU Yong, LI Hui-zhong, GAN Zi-yang, LIU Bin, HE Yue-hui. An investigation on microstructural and mechanical properties of powder metallurgical TiAl alloy during hot pack-rolling [J]. Materials Science and Engineering A, 2014, 619: 265−273.

[12] GE S, ISAC M, GUTHRIE R I L. Progress of strip casting technology for steel: Historical developments [J]. ISIJ International, 2012, 52(12): 2109−2122.

[13] GE S, ISAC M, GUTHRIE R I L. Progress in strip casting technologies for steel: Technical developments [J]. ISIJ International, 2013, 53(5): 729−742.

[14] XU Yun-bo, ZHANG Yuan-xiang, WANG Yang, LI Cheng-gang, CAO Guang-ming, LIU Zhen-yu, WANG Guo-dong. Evolution of cube texture in strip-cast non-oriented silicon steels [J]. Scripta Materialia, 2014, 87(4): 17−20.

[15] LIU Hai-tao, LIU Zhen-yu, SUN Yu, GAO Fei, WANG Guo-dong. Development of λ-fiber recrystallization texture and magnetic property in Fe−6.5wt%Si thin sheet produced by strip casting and warm rolling method [J]. Materials Letters, 2013, 91: 150−153.

[16] HAGA T, TKAHASHI K, IKAWAAND M, WATARI H. Twin roll casting of aluminum alloy strips [J]. Journal of Materials Processing Technology, 2004, 153−154(1): 42−47.

[17] JOHNSON D R, INUI H, MUTO S, OMIYA Y, YAMANAKA T. Microstructural development during directional solidification of α-seeded TiAl alloys [J]. Acta Materialia, 2006, 54(4): 1077−1085.

[18] KIM M C, OH M H, LEE J H, INUI H, YAMAGUCHI M, WEE D M. Composition and growth rate effects in directionally solidified TiAl alloys [J]. Materials Science and Engineering, A, 1997, 239−240(1): 570−576.

[19] BAREKAR N S, DAS S, FAN Z Y, CINDEREY R, CHAMPION N. Microstructural evaluation during melt conditioned twin roll casting (MC-TRC) of Al−Mg binary alloys [J]. Materials Science Forum, 2014, 790−791: 285−290.

[20] FORBORD B, ANDERSSON B, INGVALDSEN F, AUSTEVIK O, HORST J A, SKAUVIK I. The formation of surface segregates during twin roll casting of aluminium alloys [J]. Materials Science and Engineering A, 2006, 415(1−2): 12−20.

[21] XU Xiang-jun, LIN Jun-pin, WANG Yan-li, CHEN Guo-liang. On the microsegregation of Ti−45Al−(8−9)Nb−(W, B, Y) alloy [J]. Materials Letters, 2007, 61(2): 369−373.

[22] MATSUO M, HANAMURA T, KIMURA M, MASAHASHI N, MIZOGUCHI T, MIYAZAWA K. Microstructural characterization of twin-roll cast gamma titanium aluminide sheets [J]. ISIJ International, 2007, 31(3): 289−297.

[23] HANAMURA T, HASHIMOTO K. Microstructure and high temperature strength of direct-cast gamma TiAl-based alloy sheet [J]. Materials Transactions JIM, 1997, 38(7): 599−606.

[24] HANAMURA T, HASHIMOTO K. Improvement of microstructure and mechanical properties in TiB_2-doped TiAl alloy by direct sheet casting [J]. Materials Transactions JIM, 1998, 39(7): 724−730.

[25] CHEN Rui-run, ZHENG De-shuang, MA Teng-fei, DING Hong-sheng, SU Yan-qing, GUO Jing-jie, FU Heng-zhi. Effects and mechanism of ultrasonic irradiation on solidification microstructure and mechanical properties of binary TiAl alloys [J]. Ultrasonics Sonochemistry, 2017, 38: 120−133.

[26] MA Teng-fei, CHEN Rui-run, ZHENG De-shuang, GUO Jing-jie, DING Hong-sheng, SU Yan-qing, FU Heng-zhi. Influence of high-temperature hydrogen charging on microstructure and hot deformability of binary TiAl alloys [J]. Journal of Alloys and Compounds, 2017, 701: 399−407.

[27] LI Bao-hui, KONG Fan-tao, CHEN Yu-yong. Effect of yttrium addition on microstructures and room temperature tensile properties of Ti−47Al alloy [J]. Journal of Rare Earths, 2006, 24(3): 352−356.

[28] TSUYUMU T, KANENO Y, INOUE H, TAKASUGI T. Microstructural effects on moisture-induced embrittlement of isothermally forged TiAl-based intermetallic alloys [J]. Metallurgical Materials Transactions A, 2003, 34(3): 645−655.

[29] XU Wen-chen, JIN Xue-ze, HUANG Kai, ZONG Ying-ying, WU Shi-feng, ZHONG Xun-mao, KONG Fan-tao, SHAN De-bin, NUTT S R. Improvement of microstructure, mechanical properties and hot workability of a TiAl−Nb−Mo alloy through hot extrusion [J]. Materials Science and Engineering A, 2017, 705: 200−209.

[30] ZONG Ying-ying, WEN Dao-sheng, LIU Zu-yan, SHAN De-bin. γ-phase transformation, dynamic recrystallization and texture of a forged TiAl-based alloy based on plane strain compression at elevated temperature [J]. Materials Design, 2016, 91(2): 321−330.

[31] ZHANG Shu-zhi, ZHANG Chang-jiang, DU Zhao-xin, HOU Zhao-ping, LIN Peng, KONG Fan-tao, CHEN Yu-yong. Deformation behavior of high Nb containing TiAl based alloy in $\alpha+\gamma$ two phase field region [J]. Materials Design, 2016, 90: 225−229.

双辊薄带连铸制备 Ti−43Al 合金板材及其在热处理过程中的显微组织表征

徐 莽，刘国怀，李天瑞，王丙兴，王昭东

东北大学 轧制技术及连轧自动化国家重点实验室，沈阳 110819

摘 要：薄带连铸技术直接成形的特点可以实现难变形金属板材的制备并显著缩短流程。通过双辊薄带连铸技术制备尺寸为 1000 mm × 110 mm × 2 mm 的 Ti−43Al 合金板材，并对铸轧板材及热处理过程显微组织进行系统分析。由于凝固过程中冷却速率变化以及对称性生长，沿铸轧板材厚度方向出现边部柱状晶、心部等轴晶的不均匀组织，且中心区存在严重的 Al 元素偏析；铸轧过程中较快的冷却速度显著细化板材组织，晶粒间距为 20−30 μm，α_2/γ 片层间距达到 10−20 nm。此外，铸轧板材经过热处理后获得近 γ 组织、近片层组织和全片层组织，组织均匀性得到明显改善。

关键词：薄带铸轧；钛铝合金；板材制备；显微组织表征；热处理

(Edited by Xiang-qun LI)